Dalton Transactions

PAPER

View Article Online
View Journal | View Issue

Cite this: *Dalton Trans.*, 2014, **43**, 12967

Sulfonic acid-functionalized silica-coated magnetic nanoparticles as an efficient reusable catalyst for the synthesis of 1-substituted 1*H*-tetrazoles under solvent-free conditions†

Hossein Naeimi* and Samaneh Mohamadabadi

Received 5th June 2014,
Accepted 1st July 2014

DOI: 10.1039/c4dt01664e

www.rsc.org/dalton

Regarding green chemistry goals, silica-coated magnetite nanoparticles open up a new avenue to introduce a very useful and efficient system for facilitating catalyst recovery in different organic reactions. Therefore, in this paper the preparation of sulfonic acid-functionalized silica-coated magnetic nanoparticles with core–shell structure (Fe_3O_4@silica sulfonic acid) is presented by using Fe_3O_4 spheres as the core and silica sulfonic acid nanoparticles as the shell. The catalyst was characterized by infrared spectroscopy, scanning electron microscopy, X-ray diffraction analysis, dynamic light scattering, thermogravimetric analysis and vibrating sample magnetometry. Nanocatalyst can be recovered using an external magnet and reused for subsequent reactions 6 times without noticeable deterioration in catalytic activity.

Introduction

Magnetic iron oxide nanoparticles have attracted much research interest over recent years because of their unique physicochemical properties and great potential for various biomedical applications. In several pioneering works magnetic nanoparticles were claimed as an effective tool for magnetically assisted biomolecule separation,[1] biochemical sensing,[2] NMR imaging,[3,4] targeted drug delivery[5,6] and cancer treatment through hyperthermia.[7,8] The requirements for any biomedical application of magnetic nanoparticles include the chemical stability, biocompatibility, strong magnetization and low coercivity of the dispersed magnetic nanoparticles.

Tetrazoles have a wide range of applications.[9] For example, they have roles in material science including explosives and rocket propellants.[10,11] In addition, they can also function as ligands in coordination chemistry[12] and information recording systems.[13]

Tetrazoles can be prepared by several methods including acid-catalyzed cycloaddition between hydrazoic acid and isocyanides,[14] acid-catalyzed cycloaddition between isocyanides and trimethyl azide,[15] cyclization between primary amines, or their salts, with an orthocarboxylic acid ester in acetic acid or trifluoroacetic acid and sodium azide,[16] and cyclizations from an amine, triethyl orthoformate, using AcOH, PCl_5, $In(OTf)_3$, $Yb(OTf)_3$, SSA, $[HBIm]BF_4$, natrolite zeolite, chitosan-supported magnetic ionic liquid (CSMIL) and Fe_3O_4@SiO_2/salen complex of Cu(II) as catalysts.[17–25]

In this work, silica-coated magnetite nanoparticles are synthesized through two steps. The magnetite nanoparticles are firstly prepared by a co-precipitation method. Then the magnetite nanoparticles are used to synthesize Fe_3O_4@SiO_2 composite nanoparticles through the modified Stöber method.[26] The ability of this nano-magnetic solid acid to catalyze the one-pot, three-component reaction between triethyl orthoformate, an amine and sodium azide is also described. Mild reaction conditions, catalyst with high catalytic activity and good reusability, and simple magnetic work-up make this methodology an interesting option for the economic synthesis of 1-substituted 1*H*-tetrazoles under solvent-free conditions.

Results and discussion

Preparation and characterization of the catalyst

Fe_3O_4@silica sulfonic acid core–shell composite, with Fe_3O_4 spheres as the core and silica sulfuric acid nanoparticles as the shell, was prepared by a simple, low-cost and convenient method. Magnetite nanoparticles were synthesized by the co-precipitation route. To improve the chemical stability of the magnetite nanoparticles, their surfaces were successfully modified by the suitable deposition of silica onto the nanoparticle surface by the ammonia-catalyzed hydrolysis of tetraethylorthosilicate (TEOS). Next, the SiO_2 spheres served as support for

Department of Organic Chemistry, Faculty of Chemistry, University of Kashan, Kashan, 87317, IR Iran. E-mail: naeimi@kashanu.ac.ir; Fax: +98-361-5912397; Tel: +98-361-5912388

†Electronic supplementary information (ESI) available. See DOI: 10.1039/c4dt01664e

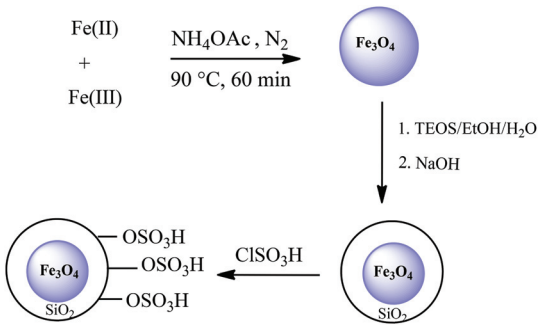

Scheme 1 Preparation steps for fabricating sulfonic acid-functionalized magnetic Fe_3O_4 nanoparticles.

the immobilization of SO_3H groups by simple mixing of core–shell composite and chlorosulfonic acid in CH_2Cl_2 (Scheme 1).

Fe_3O_4@silica sulfonic acid nanocomposite was characterized by Fourier transform infrared (FT-IR) spectroscopy, X-ray diffraction (XRD), thermogravimetric analysis (TGA), scanning electron microscopy (SEM), dynamic light scattering (DLS) and vibrating sample magnetometry (VSM).

Fig. 1 shows the FT-IR spectra of pure Fe_3O_4, Fe_3O_4@SiO_2 core–shell, and Fe_3O_4@silica sulfonic acid nanoparticles. The absorption peak at approximately 570 cm^{-1} corresponds to the stretching vibration of the Fe–O bond and the adsorption of the silica coating on the magnetite surface was indicated by the band near 1100 cm^{-1} assigned to the Si–O stretching vibration. Also, successful sulfonic acid functionalization of the silica layer on Fe_3O_4 surface was evidenced by the absorption bands at 1040 and 1130 cm^{-1} related to the stretching of the S–O bonds. A peak appeared at about 3400 cm^{-1} due to the stretching of OH groups in the SO_3H moiety (Fig. 1c). These FT-IR spectra provided evidence of the formation of a silica shell onto the surface of Fe_3O_4 and the acid functionalization of the silica shell.

Fig. 2 shows the XRD patterns of magnetic nanoparticles. The observed diffraction peaks appearing at 2θ = 30.3°, 35.6°, 43.3°, 53.8°, 57.4° and 62.9° corresponding to the diffractions

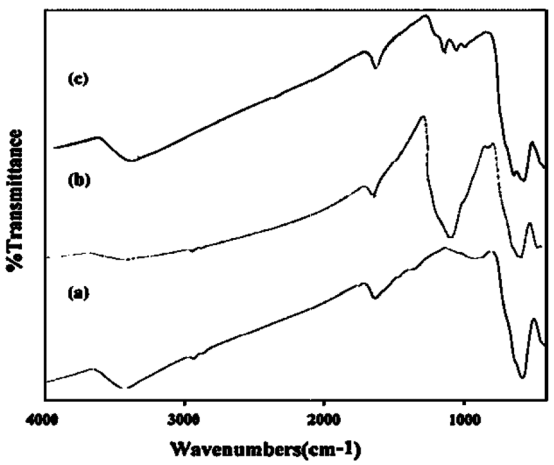

Fig. 1 Comparison of FT-IR spectra for (a) Fe_3O_4, (b) Fe_3O_4@SiO_2 and (c) Fe_3O_4@silica sulfonic acid.

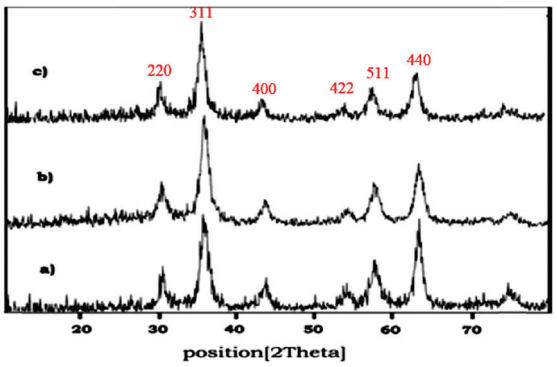

Fig. 2 XRD patterns of (a) Fe_3O_4, (b) Fe_3O_4@SiO_2 and (c) Fe_3O_4@silica sulfonic acid.

of (220), (311), (400), (422), (511) and (440) are indexed to the crystalline cubic inverse spinel structure of Fe_3O_4 nanoparticles. The sizes of the nanoparticles were evaluated from the XRD data using the Debye–Scherrer equation, which gives a relationship between particle size and peak broadening:

$$d = k\lambda/(\beta \cos \theta)$$

where d is the particle size of the crystal, k is the Scherrer constant (0.94), λ is the X-ray wavelength (0.15406 nm), β is the line broadening in radians obtained from the full width at half maximum (FWHM), and θ is the Bragg diffraction angle of the XRD diffraction peaks. The average MNPs core diameter was calculated to be 21 nm from the XRD results using the above equation.

TGA was used to study the thermal stability of the acid catalyst (Fig. 3). It is clear that, for the Fe_3O_4@silica sulfonic acid MNPs, there are three steps of weight loss. (1) Below 150 °C, there was a mass loss that was attributable to the loss of adsorbed solvent or trapped water from the catalyst. (2) Around 150–500 °C, a large weight reduction occurred, which can be mainly ascribed to the decomposition of SO_3H groups (Fig. 3b). (3) Above 500 °C, the occurrence of further mass losses at higher temperature resulted from the decomposition of the silica shell.[27]

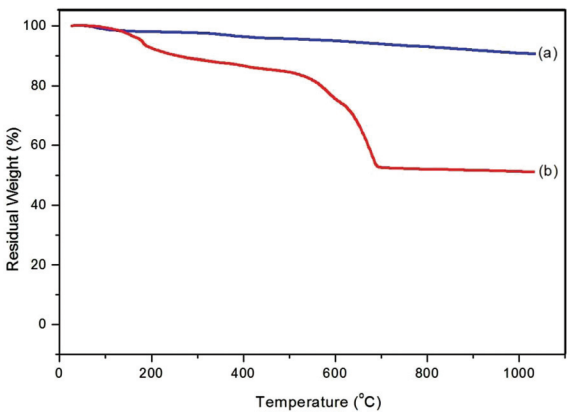

Fig. 3 TGA curves of (a) Fe_3O_4@SiO_2 and (b) Fe_3O_4@silica sulfonic acid.

The morphology and structure of prepared samples were characterized by SEM. Fig. 4a shows that the Fe_3O_4 nanoparticles are spherical in shape with an average size of 20 ± 2 nm. Fig. 4b shows that most of the Fe_3O_4@SiO_2 nanoparticles are spherical with larger particle size and smoother surface. The SEM image shown in Fig. 4c demonstrates that Fe_3O_4@silica sulfonic acid nanoparticles are approximately spherical.

The DLS measurements of Fe_3O_4@silica sulfonic acid nanoparticles are shown in Fig. 5. In order to determine the fraction of the particle population that aggregates, comparisons between the intensity-averaged DLS data and number-averaged DLS data were made. From this slurry, an aqueous stock dispersion (100 ml acetone with 5 g Fe_3O_4@silica sulfonic acid) was prepared using an ultrasonic bath for 30 min.

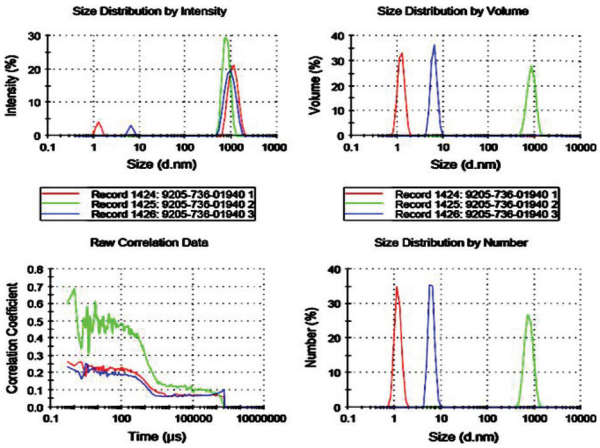

Fig. 5 DLS of Fe_3O_4@silica sulfonic acid.

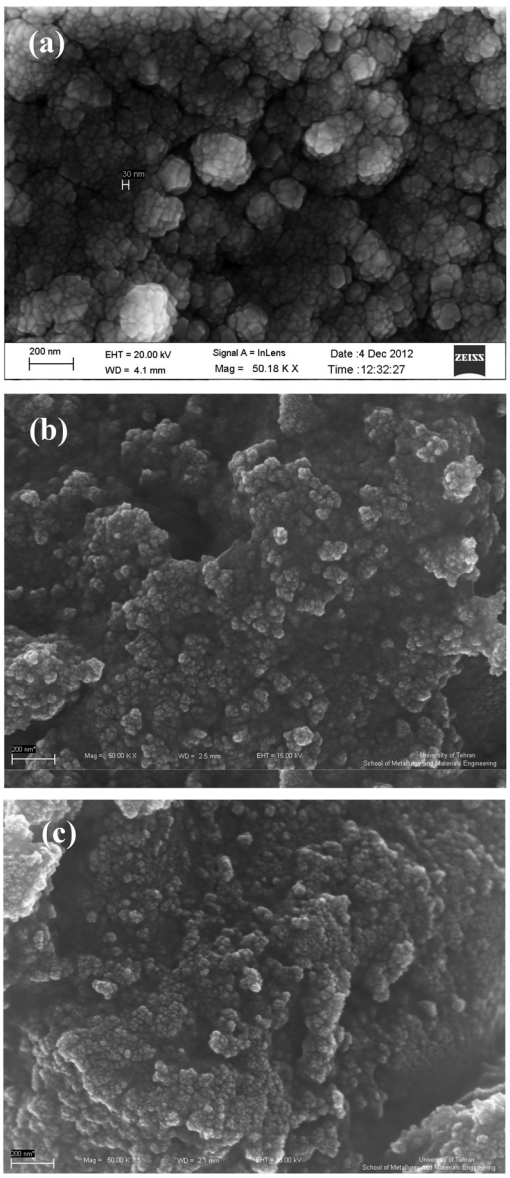

Fig. 4 SEM images of (a) Fe_3O_4, (b) Fe_3O_4@SiO_2 and (c) Fe_3O_4@silica sulfonic acid.

The magnetic property of the catalyst was studied by VSM. On the basis of Fig. 6, the saturation magnetization value was measured to be 50.86 emu g^{-1} for Fe_3O_4@SiO_2 and 14 emu g^{-1} for Fe_3O_4@silica sulfonic acid. The results show that the surface modification reaction has little impact on the magnetism of nano-adsorbent before and after modification, and also the saturation magnetization of sulfonic acid-functionalized silica-coated magnetic nanoparticles is lower than that of Fe_3O_4@SiO_2 nanoparticles. Furthermore, the number of H^+ sites (0.33 mmol g^{-1}) for Fe_3O_4@silica sulfonic acid was quantitatively determined by acid–base titration.[27]

Optimization of the reaction conditions

In further studies regarding the effect of catalyst amount on formation of 1-substituted 1*H*-tetrazoles, we found that the yields were obviously affected by the amount of catalyst. It was found that 0.02 g Fe_3O_4@silica sulfonic acid was sufficient to catalyze the reaction of 4-chloroaniline, triethyl orthoformate and sodium azide at 100 °C (Table 1, entry 4). The usage of higher amounts of catalyst did not increase the yields significantly, while decreasing the amount of catalyst reduced the yields (Table 1). Also, when the reaction was attempted without the addition of catalyst, no desired product was obtained (Table 1, entry 1).

After optimization of the reaction conditions, the reaction of triethyl orthoformate and sodium azide with various amines

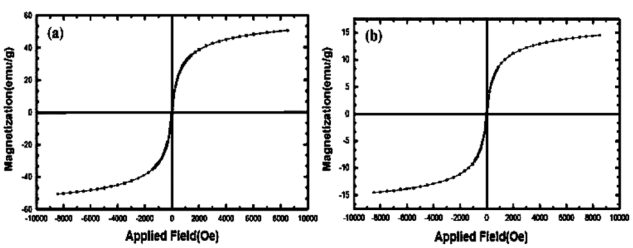

Fig. 6 Magnetization curves for the prepared (a) Fe_3O_4@SiO_2 and (b) Fe_3O_4@silica sulfonic acid.

Table 1 Effect of catalyst amount on formation of 1-substituted 1*H*-tetrazoles[a]

Entry	Cat. amount (g)	Time (min)	Yield[b] (%)
1	No catalyst	300	0
2	0.005	150	65
3	0.01	120	82
4	0.02	80	95
5	0.03	50	80
6	0.05	50	63

[a] Reaction conditions: 4-chloroaniline (1 mmol), triethyl orthoformate (1.2 mmol), and sodium azide (1 mmol). [b] Isolated yield.

was carried out according to the general experimental procedure shown in Scheme 2.

In all cases, the corresponding 1-substituted 1*H*-tetrazoles were obtained in high to excellent yields and in short reaction times. Therefore, we carried out the reaction of several anilines with triethyl orthoformate and sodium azide in the presence of 0.02 g Fe_3O_4@silica sulfonic acid. The results are summarized in Table 2.

A wide range of anilines containing electron-withdrawing groups and electron-donating groups such as bromo, chloro, methyl and acetyl underwent condensation in short reaction times with excellent isolated yields. The *para*-position anilines (Table 2, entries 3 and 4) gave good results in comparison to the *ortho*-position anilines (Table 2, entries 6 and 10). There is more steric hindrance for the *ortho*-position anilines (*o*-Cl, -Me) on product formation than the *para*-position (*p*-Cl, -Me) anilines. All known compounds were characterized by comparing their physical and spectral data with those reported in the literature.

Reusability of the catalyst

The reusability is one of the important properties of this catalyst. The possibility of recovery of the catalyst was investigated for the reaction of aniline, triethyl orthoformate, and sodium azide under optimized conditions. After completion of the model reaction, the catalyst was recovered from the reaction mixture simply by an external magnet. Then the recovered catalyst was washed with ethyl acetate, and reused for subsequent reactions 6 times without noticeable deterioration in catalytic activity (Fig. 7).

Comparison of the Fe_3O_4@silica sulfonic acid catalyst with other catalysts

In subsequent experiments, the activity of the prepared catalyst was measured in the model reaction. From Table 3, it is clear that Fe_3O_4@silica sulfonic acid worked remarkably well to give the desired product within 50 min in 97% yield in shorter reaction time and lower temperature than SSA and natrolite zeolite. Also this catalyst is comparable with $In(OTf)_3$, [HBIm]-BF_4, CSMIL and Fe_3O_4@SiO_2/salen Cu(II).

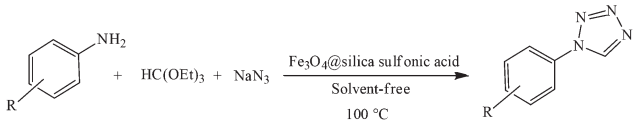

Scheme 2 Synthesis of 1-substituted 1*H*-tetrazoles catalyzed by Fe_3O_4@silica sulfonic acid.

Experimental section

Chemicals

Iron(II) chloride tetrahydrate (99%), iron(III) chloride hexahydrate (98%), tetraethoxysilane (TEOS), chlorosulfonic acid and other chemical materials were purchased from Fluka and Merck and used without further purification.

Apparatus

Products were characterized by comparison of their physical data, and IR, ^{1}H NMR and ^{13}C NMR spectra with known samples. NMR spectra were recorded with a Bruker Advance DPX 400 MHz spectrometer at 400 and 100 MHz in $CDCl_3$ as solvent in the presence of TMS as internal standard. IR spectra were recorded as KBr pellets using a Perkin-Elmer 781 spectrophotometer. The purity determination of the products and reaction monitoring were accomplished by thin-layer chromatography (TLC) on silica gel PolyGram SILG/UV 254 nm plates. XRD patterns of samples were obtained with a Philips Xpert X-ray powder diffractometer (CuK radiation, k = 0.154056 nm). The particle morphology was examined by SEM (Hitachi S4160 scanning electron microscope). TGA patterns were obtained for characterization of the heterogeneous catalyst with a Rheometric Scientific Inc. 1998 thermal analysis apparatus under a N_2 atmosphere. DLS was performed with a Malvern ZEN 3600. Melting points were measured using a Yanagimoto micro melting point apparatus. A Bandelin ultrasonic HD 3200 with probe model KE of 76.6 mm in diameter was used to produce ultrasonic irradiation.

Preparation of Fe_3O_4 (MNPs)

Magnetic nanoparticles were synthesized by co-precipitation of $FeCl_3{\cdot}6H_2O$ and $FeCl_2{\cdot}4H_2O$ in ammonia solution, according to a reported procedure.[27,28] Typically, $FeCl_3{\cdot}6H_2O$ (15.136 g) and $FeCl_2{\cdot}4H_2O$ (6.346 g) were dissolved in 0.64 L deionized water under nitrogen at 90 °C and added to a 25% ammonium hydroxide solution (0.08 L) with vigorous mechanical stirring. After the color of the bulk solution turned to black the reaction was carried out for 60 min in N_2 atmosphere. The resulting black MNPs were isolated by applying an external magnet, washed 3 times with deionized water and then dried under vacuum at 60 °C for 12 h.

Preparation of Fe_3O_4@SiO_2

The Fe_3O_4@SiO_2 nanospheres were prepared by a modified Stöber method. Briefly, Fe_3O_4 (0.50 g) was dispersed in a mixture of ethanol (50 mL), deionized water (5 mL) and TEOS (0.20 mL), followed by the addition of 5.0 mL of NaOH (10 wt%). This solution was stirred mechanically for 30 min

Table 2 Preparation of 1-substituted 1*H*-tetrazoles in the presence of Fe_3O_4@silica sulfonic acid[a]

Entry	Substrate	Product	Time (min)	Yield[b] (%)	TON
1	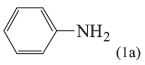 (1a)	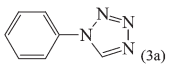 (3a)	50	97	146.96
2	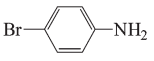 (1b)	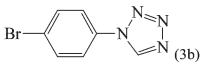 (3b)	80	95	143.94
3	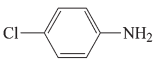 (1c)	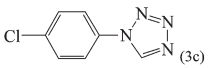 (3c)	80	95	143.94
4	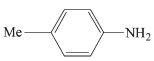 (1d)	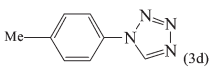 (3d)	60	92	139.39
5	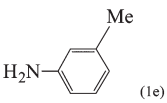 (1e)	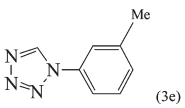 (3e)	70	87	131.81
6	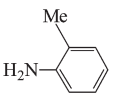 (1f)	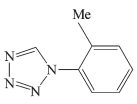 (3f)	100	82	124.24
7	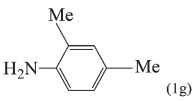 (1g)	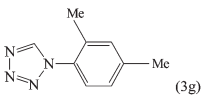 (3g)	90	90	136.36
8	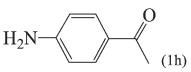 (1h)	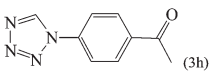 (3h)	180	78	118.18
9	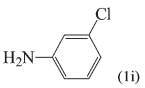 (1i)	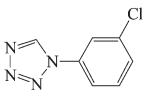 (3i)	100	96	151.51
10	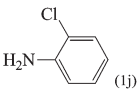 (1j)	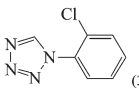 (3j)	135	83	125.75
11	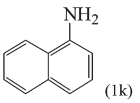 (1k)	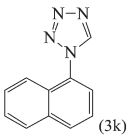 (3k)	150	84	127.27
12	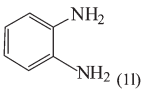 (1l)	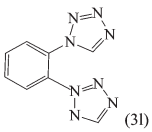 (3l)	170	81	122.72

[a] Reaction conditions: amines (1 mmol), triethyl orthoformate (1.2 mmol), and sodium azide (1 mmol). [b] Isolated yield.

at room temperature. Then the product, Fe_3O_4@SiO_2, was separated by an external magnet and was washed with deionized water and ethanol three times and dried at 80 °C for 10 h.

Preparation of Fe_3O_4@silica sulfonic acid

A suction flask was equipped with a constant pressure dropping funnel. The gas outlet was connected to a vacuum system through an adsorbing solution of alkali trap. Fe_3O_4@silica (0.5 g) was added into the flask and dispersed ultrasonically for 10 min in dry CH_2Cl_2 (10 mL). Chlorosulfonic acid (0.4 mL) was added dropwise to a cooled ice-bath over a period of 30 min at room temperature. After completion of the addition, the mixture was shaken for 90 min, while the residual HCl was eliminated by suction. Then the Fe_3O_4@silica sulfonic acid was separated from the reaction mixture by a magnetic field and washed several times with dried CH_2Cl_2. Finally, Fe_3O_4@silica sulfonic acid was dried under vacuum at 60 °C.

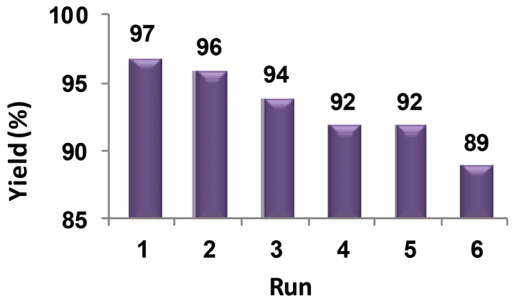

Fig. 7 Reusability of Fe_3O_4@silica sulfonic acid for the reaction of aniline, triethyl orthoformate, and sodium azide under solvent-free conditions.

Table 3 Comparison of different catalysts in the formation of 1-substituted 1*H*-tetrazoles[a]

Entry	Catalyst	Solvent	Temp. (°C)	Time (min)	Yield[b] (%)	Ref.
1	SSA	Neat	120	300	95	20
2	Natrolite zeolite	Neat	120	240	82	22
3	$In(OTf)_3$	Neat	100	90	89	18
4	$[HBIm]BF_4$	Neat	100	30	91	21
5	CSMIL	Neat	70	60	92	23
6	Fe_3O_4@SiO_2/salen Cu(II)	Neat	100	60	96	24
7	Fe_3O_4@silica sulfonic acid	Neat	100	50	97	—

[a] Reaction conditions: aniline (1 mmol), triethyl orthoformate (1.2 mmol), and sodium azide (1 mmol), Fe_3O_4@silica sulfonic acid (0.02 g), solvent free at 100 °C. [b] Isolated yield.

General synthesis for the preparation of 1-substituted 1*H*-tetrazoles

A mixture of amine (1 mmol), sodium azide (1 mmol), triethyl orthoformate (1.2 mmol) and Fe_3O_4@silica sulfonic acid (0.02 g) was placed in a round-bottomed flask and stirred at 100 °C. The progress of the reaction was monitored by TLC. After completion of the reaction, the reaction mixture was cooled to room temperature and diluted with ethyl acetate (3 × 20 mL). The catalyst was removed by an external magnet, and then the resulting solution was washed with water and dried over anhydrous Na_2SO_4. After concentration, a crystallization step was performed using EtOAc–hexane (1 : 9). The products were characterized by ^{1}H NMR, ^{13}C NMR, FT-IR and melting points. We report the spectral data of the synthesized compounds.

1-(Phenyl)-1*H*-tetrazole (3a). Yellow solid (97% yield); m.p. = 63–65 °C; M.P.$_{Lit}$: 65–67 °C; IR (KBr)/ν (cm^{-1}): 3126 (C–H, sp^2 stretch Ar), 1694 (C=N), 1597, 1498 (C=C); ^{1}H NMR ($CDCl_3$, 400 MHz) δ (ppm): 7.07–7.34 (m, 5H, Ar), 8.20 (s, 1H tetrazole).

1-(4-Bromophenyl)-1*H*-tetrazole (3b). White solid (95% yield); m.p. = 169–170 °C; IR (KBr)/ν (cm^{-1}): 3060 (C–H, sp^2 stretch, Ar), 1659 (C=N), 1576, 1482 (C=C); ^{1}H NMR ($CDCl_3$, 400 MHz) δ (ppm): 6.92–6.94 (d, 2H), 7.40–7.42 (d, 2H), 8.09 (s, 1H tetrazole); ^{13}C NMR ($CDCl_3$, 100 MHz) δ (ppm): 116.43, 120.76, 132.03, 143.99, 149.29.

1-(4-Chlorophenyl)-1*H*-tetrazole (3c). White solid (95% yield); m.p. = 153–155 °C; M.P.$_{Lit}$: 155–156 °C; IR (KBr)/ν (cm^{-1}): 3057 (C–H, sp^2 stretch, Ar), 1661 (C=N), 1485, 1581 (C=C); ^{1}H NMR ($CDCl_3$, 400 MHz) δ (ppm): 6.98–7.00 (d, 2H), 7.27–7.29 (d, 2H), 8.09 (s, 1H tetrazole); ^{13}C NMR ($CDCl_3$, 100 MHz) δ (ppm): 120.35, 128.85, 129.47, 143.52, 149.50.

1-(4-Methylphenyl)-1*H*-tetrazole (3d). Light yellow solid (87% yield); m.p. = 92–99 °C; IR (KBr)/ν (cm^{-1}): 3022 (C–H, sp^2 stretch, Ar), 2918 (C–H, sp^3 stretch), 1664 (C=N), 1607, 1506 (C=C); ^{1}H NMR ($CDCl_3$, 400 MHz) δ (ppm): 2.34 (s, 3H), 6.94–6.96 (d, 2H), 7.11–7.13 (d, 2H), 8.17 (s, 1H tetrazole); ^{13}C NMR ($CDCl_3$, 100 MHz) δ (ppm): 20.79, 119.08, 129.63, 130.17, 142.95, 149.77.

1-(3-Methylphenyl)-1*H*-tetrazole (3e). White solid (85% yield); m.p. = 53–55 °C; IR (KBr)/ν (cm^{-1}): 3167 (C–H, sp^2 stretch, Ar), 2923 (C–H, sp^3 stretch), 1690 (C=N), 1594, 1483 (C=C); ^{1}H NMR ($CDCl_3$, 400 MHz) δ (ppm): 2.33 (s, 3H), 6.86 (s, 1H), 6.89–6.91 (d, 2H), 7.18–7.22 (t, 1H), 8.21 (s, 1H tetrazole); ^{13}C NMR ($CDCl_3$, 100 MHz) δ (ppm): 21.43, 115.93, 119.97, 124.06, 129.19, 139.26, 145.28, 149.23.

1-(2-Methylphenyl)-1*H*-tetrazole (3f). White solid (82% yield); m.p. = 152–155 °C; IR (KBr)/ν (cm^{-1}): 3015 (C–H, sp^2 stretch, Ar), 2870 (C–H, sp^3 stretch), 1664 (C=N), 1488, 1590 (C=C); ^{1}H NMR ($CDCl_3$, 400 MHz) δ (ppm): 2.33 (s, 3H), 7.02–7.03 (d, 1H), 7.05–7.07 (d, 1H), 7.18–7.22 (t, 2H), 8.08 (s, 1*H*-Tetrazole); ^{13}C NMR ($CDCl_3$, 100 MHz) δ (ppm): 17.94, 117.68, 123.43, 127, 128.71, 130.72, 144.10, 147.78.

1-(2,4-Dimethylphenyl)-1*H*-tetrazole (3g). White solid (90% yield); m.p. = 133–135 °C; IR (KBr)/ν (cm^{-1}): 3069 (C–H, sp^2 stretch, Ar), 2914 (C–H, sp^3 stretch), 1663 (C=N), 1495, 1607 (C=C); ^{1}H NMR ($CDCl_3$, 400 MHz) δ (ppm): 2.29 (s, 3H), 2.30 (s, 3H), 6.94–6.96 (d, 1H), 6.98–7.00 (d, 1H), 7.02 (s, 1H), 8.00 (s, 1H tetrazole).

1-(4-Acetylphenyl)-1*H*-tetrazole (3h). Yellow solid (78% yield); m.p. = 175–176 °C; IR (KBr)/ν (cm^{-1}): 3075 (C–H, sp^2 stretch, Ar), 2995 (C–H, sp^3 stretch), 1669 (C=N), 1499, 1585 (C=C); ^{1}H NMR ($CDCl_3$, 400 MHz) δ (ppm): 2.60 (S, 3H), 7.13–7.15 (d, 2H), 7.95–7.97 (d, 2H), 8.30 (s, 1H tetrazole).

1-(3-Chlorophenyl)-1*H*-tetrazole (3i). White solid (81% yield); m.p. = 137–139 °C; IR (KBr)/ν (cm^{-1}): 3065 (C–H, sp^2 stretch, Ar), 1669 (C=N), 1473, 1586 (C=C); ^{1}H NMR ($CDCl_3$, 400 MHz) δ (ppm): 6.92–6.94 (d, 1H) 7.07–7.09 (d, 2H) 7.26–7.27 (t, 1H), 8.14 (s, 1H tetrazole); ^{13}C NMR ($CDCl_3$, 100 MHz) δ (ppm): 117.45, 119.23, 123.73, 130.34, 135.12, 146.14, 149.72.

1-(2-Chlorophenyl)-1*H*-tetrazole (3j). White solid (79% yield); m.p. = 129–131 °C; IR (KBr)/ν (cm^{-1}): 3023 (C–H, sp^2 stretch, Ar), 1670 (C=N), 1481, 1598 (C=C); ^{1}H NMR ($CDCl_3$, 400 MHz) δ (ppm): 7.03–7.50 (m, 4H), 8.10 (s, 1H tetrazole).

1-(Naphthalen-1-yl)-1*H*-tetrazole (3k). White solid (84% yield); m.p. = 132–135 °C; IR (KBr)/ν (cm^{-1}): 3048 (C–H, sp^2 stretch, Ar), 1658 (C=N), 1574, 1432 (C=C); ^{1}H NMR ($CDCl_3$, 400 MHz) δ (ppm): 7.23–8.27 (m, 7H), 8.36 (s, 1H tetrazole).

1-[2-(1*H*-Tetrazol-1-yl)phenyl]-1*H*-tetrazole (3l). White solid (83% yield); m.p. = 167–169 °C; IR (KBr)/ν (cm^{-1}): 3062 (C–H, sp^2 stretch, Ar), 1619 (C=N) 1458, 1588 (C=C); ^{1}H NMR ($CDCl_3$, 400 MHz) δ (ppm): 7.30–7.70 (m, 4H), 8.11 (s, 1H tetrazole); ^{13}C NMR ($CDCl_3$, 100 MHz) δ (ppm): 115.76, 122.37, 138.50, 142.40.

Conclusion

In conclusion, we have firstly reported that Fe_3O_4@silica sulfonic acid can be an efficient and reusable catalyst for one-pot synthesis of 1-substituted 1*H*-tetrazoles from an amine, triethyl orthoformate and sodium azide. The catalytic research on novel approaches toward magnetic nanoparticles should be improved to enhance organic synthesis. For that purpose, the magnetic nanocatalyst provides a high surface area for interaction with compounds. This catalyst can provide a new way for continuous processes, because of its simple recyclability. Good yields, short reaction times, solvent-free conditions, non-toxicity and recyclability with a very easy operation are the most important advantages of the synthesized catalyst. The catalyst can be easily recovered from the reaction system by an external magnet and reused 6 times without noticeable deterioration in catalytic activity.

Acknowledgements

The authors are grateful to University of Kashan for supporting this work by grant no. 159148/43.

Notes and references

1 O. Olsvik, T. Popovic, E. Skjerve, K. S. Cudjoe, E. Hornes, J. Ugelstad and M. Uhlen, *Clin. Microbiol. Rev.*, 1994, **7**, 43–54.
2 M. N. Widjojoatmodjo, A. C. Fluit, R. Torensma and J. Verhoef, *J. Immunol. Methods*, 1993, **165**, 11–19.
3 R. Weissleder, G. Elizondo, J. Wittenberg, C. A. Rabito, H. H. Bengele and L. Josephson, *Radiology*, 1990, **175**, 489–493.
4 J. W. M. Bulte, L. D. Ma, R. L. Magin, R. L. Kamman, C. E. Hulstaert, K. G. Go, T. H. The and L. de Leij, *Magn. Reson. Med.*, 1993, **29**, 32–37.
5 P. K. Gupta, C. T. Hung, F. C. Lam and D. G. Perrier, *Int. J. Pharm.*, 1988, **43**, 167–177.
6 T. Neuberger, B. Schöpf, H. Hofmann, M. Hofmann and B. von Rechenberg, *J. Magn. Magn. Mater.*, 2005, **293**, 483–496.
7 A. Jordan, P. Wust, H. Fahling and R. Scholz, *Int. J. Hyperthermia*, 1993, **9**, 51–58.
8 U. Hafeli, W. Schutt, J. Teller and M. Zborowski, *Scientific and Clinical Applications of Magnetic Carriers*, Plenum Press, New York and London, 1997, pp. 527–534.
9 R. N. Butler and A. R. Katritzky, in *Comprehensive Heterocyclic Chemistry*, ed. C. W. Rees and E. F. V. Scriven, Pergamon, Oxford, UK, 1996, vol. 4.
10 (*a*) V. A. Ostrovskii, M. S. Pevzner, T. P. Kofmna, M. B. Shcherbinin and I. V. Tselinskii, *Targets Heterocycl. Syst.*, 1999, **3**, 467; (*b*) M. Hiskey, D. E. Chavez, D. L. Naud, S. F. Son, H. L. Berghout and C. A. Bome, *Proc. Int. Pyrotech. Semin.*, 2000, **27**, 3.
11 M. U. S. Brown, *Patent* 3,338,915, 1967; *Chem. Abstr.*, 1968, 87299.
12 (*a*) V. V. Nilulin, T. V. Artamonova and G. I. Koldobskii, *Russ. J. Org. Chem.*, 2003, **39**, 1525–1529; (*b*) V. V. Nilulin, T. V. Artamonova and G. I. Koldobskii, *Russ. J. Org. Chem.*, 2005, **41**, 444–445.
13 G. I. Koldobskii and V. A. Ostrovskii, *Usp. Khim.*, 1994, **63**, 847.
14 (*a*) D. M. Zimmerman and R. A. Olofson, *Tetrahedron Lett.*, 1969, **58**, 5081; (*b*) F. G. Fallon and R. M. Herbst, *J. Org. Chem.*, 1957, **22**, 933.
15 T. Jin, S. Kamijo and Y. Yamamoto, *Tetrahedron Lett.*, 2004, **45**, 9435.
16 Y. Satoh and N. Marcopulos, *Tetrahedron Lett.*, 1995, **36**, 1759–1762.
17 A. K. Gupta and C. H. Oh, *Tetrahedron Lett.*, 2004, **45**, 4113–4116.
18 K. Dhiman, M. Adinath and H. Alakananda, *Tetrahedron Lett.*, 2009, **50**, 2668–2670.
19 W. Su, Z. Hong, W. Shan and X. Zhang, *Eur. J. Org. Chem.*, 2006, 2723–2726.
20 D. Habibi, H. Nabavi and M. Nasrollahzadeh, *J. Chem.*, 2012, 1–4.
21 T. M. Potewar, S. A. Siddiqui, R. J. Lahoti and K. V. Srinivasan, *Tetrahedron Lett.*, 2007, **48**, 1721–1724.
22 D. Habibi, M. Nasrollahzadeh and T. A. Kamali, *Green Chem.*, 2011, **13**, 3499–3504.
23 A. khalafi-Nezhad and S. mohammadi, *RSC Adv.*, 2013, **3**, 4362–4371.
24 F. Dehghani, A. R. Sardarian and M. Esmaeilpour, *J. Organomet. Chem.*, 2013, **743**, 87–96.
25 N. T. Pokhodylo, V. S. Matiychuk and M. D. Obushak, *Tetrahedron*, 2008, **64**, 1430.
26 W. Stöber, A. Fink and E. Bohn, *J. Colloid Interface Sci.*, 1968, **26**, 62–69.
27 F. Nemati, M. M. Heravi and R. Saeedirad, *Chin. J. Catal.*, 2012, **33**, 1825–1831.
28 K. D. Kim, S. S. Kim, Y. H. Choa and H. T. Kim, *J. Ind. Eng. Chem.*, 2007, **13**, 1137–1141.